

Relationship between Mechanical Properties and Porosity of Porous Polymer Sheet Fabricated using Water-soluble Particles

Sae-Rom So*, Suk-Hee Park** and Sang-Hu Park***,#

*Graduate School of Mechanical Engineering, Pusan National University,

**Korea Institute of Industrial Technology(KITECH)

***School of Mechanical Engineering/ERC-NSDM, Pusan National University,

수용성 입자를 이용한 다공성 폴리머 구조체의 공극률 향상과 기계적 물성과의 관계

소새롬*, 박석희**, 박상후***,#

*부산대학교 기계공학부 대학원, **한국생산기술연구원 제조혁신센터,

***부산대학교 기계공학부/정밀정형 및 금형가공연구소

(Received 20 August 2018; received in revised form 5 September 2018; accepted 7 September 2018)

ABSTRACT

A polymer porous sheet, which can be applied to diverse wearable devices, has some advantages such as light-weight, high flexibility, high elongation, and so many others. In order to fabricate a porous sheet, water-soluble particles like sugar were utilized frequently, and there has been great advances. However, with our best knowledge, there are not enough reports on the mechanical behavior of porous sheets having different porosity. So, in this work, we tried to find out the relationship between porosity and mechanical deformation of a porous sheet. The process parameters such as a particle size, sheet thickness and PDMS mixing ratio with curing agent were analyzed on the effect of increasing the porosity of a sheet. Also, mechanical deformation of a sheet was tested using a tensile experiment. Through the experimental results, we make a conclusion that a highly porous sheet with thin thickness has high flexibility, and it deformed nearly double elongation comparing to worst one among nine cases.

Key Words : Porous Sheet(다공성 판재), 3D Printing(3D 프린팅), Porosity(공극률), Flexible Sensor(유연 센서)

1. Introduction

In general, porous structure sheets consist of irregular and various sizes of pores, both internally

and externally. The porous sheets that are made of polymer materials are characterized by flexibility and light weight,^[1] whereas those made of metallic materials are widely applied to structural materials, creating high stiffness relative to weight.^[2] The porous materials are also used as functional materials, such as porous sponges,^[3-4] to solve the

Corresponding Author : sanghu@pusan.ac.kr

Tel: +82-51-510-1011, Fax: +82-51-510-1973

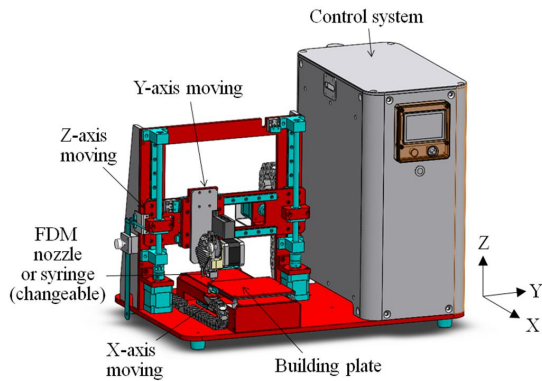


Fig. 1 CAD image of developed 3D printer that prints a frame using double material like filament and liquid PDMS

problem of marine pollution caused by oil spills. In addition, the porous structure is also used as a high-elongation substrate of wearable sensors.^[5-6] The additive manufacturing industry also uses porous structures to make functional structures.^[7]

Among the methods of making polymer porous structures, the methods using a 3D printer and mixing water-soluble particles, such as sugar with a medium, are widely used. The method of using 3D printers has been used as a method of making biometric scaffolding^[10] for cell culture through patterned and ordered,^[8] or irregular, porous structures.^[9] It is also a method of making patient-customized devices.^[11] In the case of regular porous structure, it is easy to implement desired characteristics by changing and adjusting the size and direction of the pores according to the purpose of study. However, adjusting the pore size to micro level is difficult, and expensive equipment is required.

On the contrary, an irregular porous structure is easy to make, but it is difficult to obtain uniform physical properties. This is because the mechanical properties of the sheets are changed depending on the size, arrangement, and shape of the pores. The method using water-soluble particles, such as sugar,

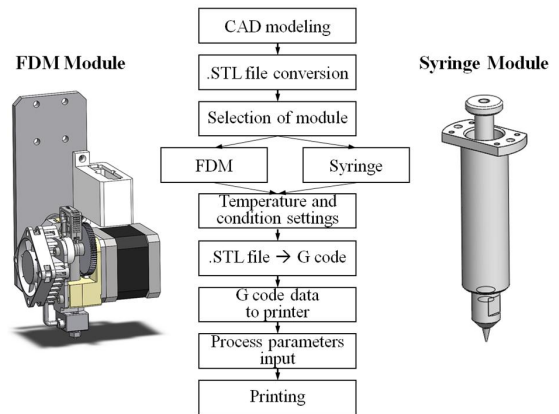


Fig. 2 Flow chart of printing process and two modules of FDM and syringe

has the advantage of being able to easily make the porous structure. Such porosity is directly related to the physical properties of the sheets, as described above. In particular, flexibility, which is important for the production of flexible devices, is highly correlated with porosity.

Unfortunately, there have been few cases of making flexible porous sheets that are suitable for application purposes. Therefore, this study made porous sheets by adjusting sugar powder for porosity adjustment, and analyzed the correlation with the porosity. In addition, this study produced a frame using a 3D printer and a porous sheet using sugar powder and PDMS (polydimethylsiloxane, Sylgard-184, Dow Corning Co., USA).

This study also monitored the change in viscosity according to the size of sugar powder particles and mixing ratio of the PDMS curing agent, as well as the change in porosity according to the thickness of the sheet.

2. Experiment Method

2.1 3D-Printing Device Configuration

In order to produce a flat and curved frame, this

study configured a 3D-printing device using a mixed form of fused deposition modeling (FDM), a filament wire application method, and a syringe method that can irradiate liquid materials, as shown in Fig. 1.

As shown in Fig. 2, this device is operated in a stepwise manner, such as when two modules are selected to produce a frame, and when PDMS is put in. This study produced a desired form of an outer frame with polyvinyl alcohol (PVA) filament materials, using the FDM method mixed with a water-soluble powder. Next, the curing agent and PDMS, mixed to form a certain ratio, were made to be discharged into the powder inside the frame to make sure that the same conditions can be implemented when fabricating the frame again in the future. To produce a flat frame for creating a porous sheet specimen, this study used the FDM module, of which detailed production conditions are summarized in Table 1.

Sugar was used as water-soluble powder and, as shown in Table 2, the sugar particle size was grouped into three categories: 200 μm or less, 200~300 μm , and 300 μm or more, using a mesh. Fifty powders in each category were measured using a microscope to average their sizes. As the sugar particles have various polygon shapes, rather than spherical shapes, the size of each particle has the

Table 1 Fabrication conditions of a frame

Process conditions	
- Printing Type	FDM
- Nozzle diameter	0.4 mm
- Temperature	220°C
- Material	PVA
- Layer thickness	0.1 mm

Table 2 Range of sugar particle size

Three ranges of particle size (μm)			
size range	~200	200~300	300~
average size	93.9	252.8	634.3

Table 3 Taguchi parameters and levels

Parameters	Levels			Unit
	1	2	3	
Size of sugar particle(α)	~200	200~300	300~	μm
Thickness of sheet(β)	2	4	6	mm
Mixing ratio of PDMS(γ)	6:1	9:1	10:1	A:B

value of $(\text{max.} + \text{min.})/2$, established as the representative size.

2.2 Process Parameter for Factor-Effect Analysis

To more precisely analyze the effects of porous sheets on porosity, this study used factor-effect analysis of Taguchi. As shown in Table 3, size of water-soluble powder particles, thickness of the sheet, and mixing ratio (A:B) of PDMS (A), and a curing agent (B), were used as parameters.

Because the viscosity changes according to the PDMS mixing ratio, it was included in process parameters, assuming that it exerts an effect on mechanical properties and porosity of porous sheets after the production.

A ratio of 10:1 was selected for this study, which is the mixing ratio with commonly used curing agent, 9:1, which showed the highest elastic modulus in precedent studies, and 6:1, which showed low viscosity as a mixing ratio.^[12]

3. Production of Porous Sheets

3.1 Production Process of Porous Sheets in Flat Structure

The production process of porous sheets in this study was as follows: First, a frame like Fig. 3(a) was produced using 3D printer with the FDM method. Water-soluble PVA materials were used in this study. The frame plays the role of maintaining

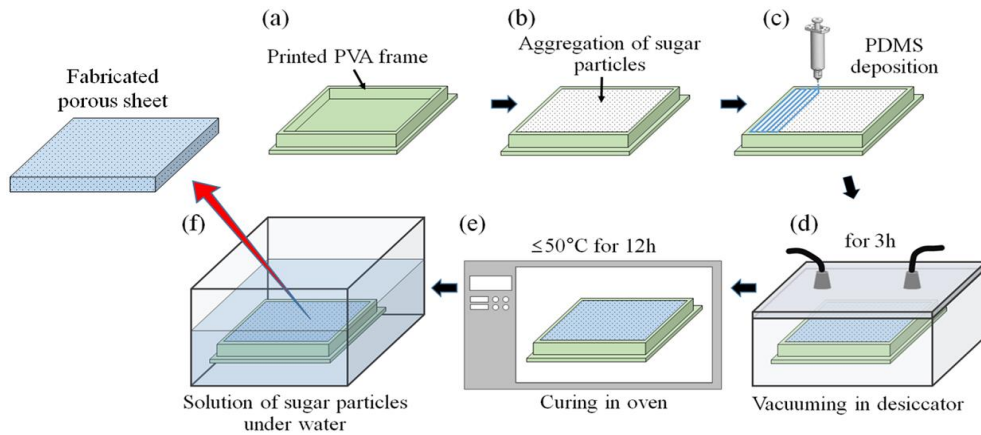


Fig. 3 Schematic diagram of fabrication process of a porous sheet using water-soluble particles

the whole size or shape of the porous sheets. To make the separation from the sheet easy, water-soluble materials were used to ensure easy separation of the frame from the sheet without damage. Next, water-soluble sugar particles of a certain size were added to the produced frame, as shown in Fig. 3(b). At this time, all of the particles must be connected to each other so that they can be completely removed when they are dissolved with water later, maximizing the porosity. A small amount of water was added to make sure the particles could be easily combined. Then, the surface was coated in PDMS mixed with a curing agent, using the syringe module of the 3D printer (see Fig. 3(c)). It was then put into a vacuum desiccator to remove bubbles that occurred in the PDMS curing process and make the PDMS easily permeate between the sugar particles. The vacuum was cleared slowly until it reached an atmospheric pressure state and stabilized the surface of the porous sheet in a horizontal state (see Fig. 3(d)).

As a final step, as shown in Figs. 3(e) and 3(f), the PDMS was cured in an oven and put into water to produce a final porous sheet by melting the water-soluble frame and sugar particles. At this time, it is necessary to carry out the curing for a long time at a temperature of 50°C or lower, which

is lower than the PDMS curing temperature of 70–80°C that is generally used, because the sugar particles may melt at the PDMS curing temperature.

Figs. 4(a)–4(d) show the porous sheets produced according to the above-mentioned three sugar particle

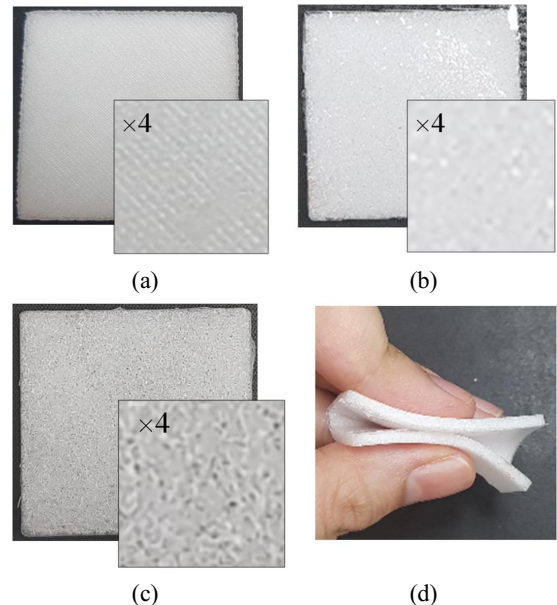


Fig. 4 Fabrication results of porous sheet based on the proposed method under diverse particle sizes of (a) $\leq 150 \mu\text{m}$, (b) $200\sim 300 \mu\text{m}$, (c) $\geq 300 \mu\text{m}$, and (d) completely folded shape

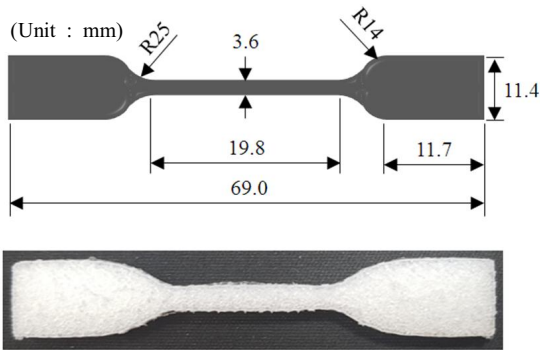


Fig. 5 Dimension of tensile specimen and fabricated image one

sizes. The sheet size was 40×40 mm, and the thickness was 2 mm. It was found that the produced porous sheet could be folded by hand because it was flexible without any defect (see Fig. 4 (d)).

3.2 Tensile-Specimen Production Process

This study produced a specimen for tensile test to find the difference in mechanical deformation behavior according to the porosity of porous sheet. The tensile-specimen production process is the same as the one shown in Figs. 3(a)–3(f). The specimen was produced in accordance with ASTM 412-D^[13] and reduced to 60% of the actual specimen size to fit the size of tensile testing machine. Fig. 5 shows the tensile-specimen specs and specimens produced.

4. Results and Discussion

4.1 Porosity Factor-Effect Analysis

This study conducted a factor-effect analysis of the process parameters for porosity shown in Table 3, Section 2.2, and examined the contribution of three parameters to maximize the porosity according to the L9 orthogonal array described in Table 4.^[14] The porosity of the porous sheet produced, according to nine production conditions, was

Table 4 Process parameters in each case

Case	α (μm)	β (mm)	Υ (A:B)
1	~200	2	6:1
2	~200	4	9:1
3	~200	6	10:1
4	200~300	2	9:1
5	200~300	4	10:1
6	200~300	6	6:1
7	300~	2	10:1
8	300~	4	6:1
9	300~	6	9:1

Table 5 Internal volume and porosity of each case

Case No.	Volume of void, V_{in} (mm^3)	Porosity $(V_{in}/V) \times 100(\%)$
1	3281.13	42.7
2	4848.88	45.1
3	5984.63	46.6
4	2433.27	35.1
5	3269.27	26.1
6	3708.03	24.3
7	1995.47	29.8
8	2393.51	28.3
9	2811.15	25.5

photographed at a spacing of $38 \mu\text{m}$ in the thickness direction of the porous sheet using computed tomography (CT, Micro Focus 3D CT System, Nikon, Japan) to create a 3D shape. The porosity of the 3D internal shape photographed in this way was calculated using the Volume Graphics Studio (VG Studio ver. 2.0, Volume Graphics, Germany) program.

As shown in Figs. 6(a)–6(i), there are some cases where the computed-tomographic image of the inside of the porous sheet was not properly photographed (see arrows in Figs. 6[a]–6[c]). These were excluded to reduce the error in porosity calculation.

Fig. 7 shows the result of factor-effect analysis using MINITAP (v.16.1.1) using porosity calculated from CT image as summarized in Table 5.

The analysis result showed that the particle of the water-soluble powder is the factor that has the

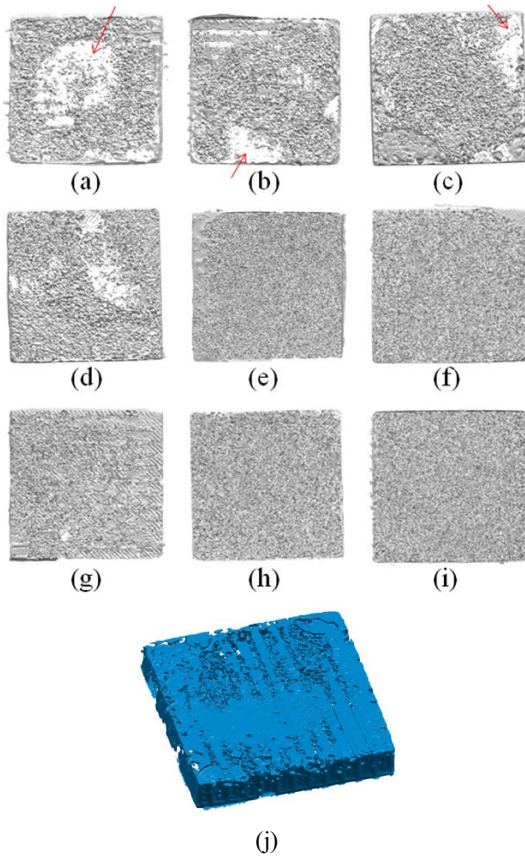


Fig. 6 (a)~(i), CT images of middle layer of nine fabrication cases; red arrows indicate mis-taken areas, and (j) assembled 3D image of porous sheet (Case No. 3)

greatest effect and the particle size of 150 μm or less showed sharp increase in porosity.

In addition, the thinner the sheet, the higher porosity it showed. In the case of the thick sheet, a lot of water-soluble powders enter into the sheet and the powders are partially fused with each other, or the PDMS is not completely permeated. So the uniformity tends to be lowered. The viscosity conditions represented by the mixing ratio of the PDMS and curing agent do not seem to have a significant difference. The above results show that porosity is greatly influenced by water-soluble

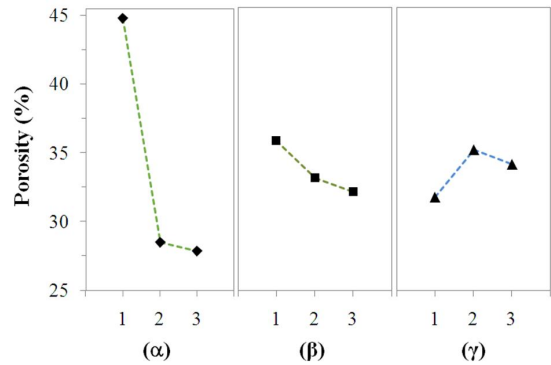


Fig. 7 Analysis results of main effects of process parameters on porosity

powder particles, and that the optimal combination for maximum porosity is a mixture of sugar powder of less than 150 μm , a thickness of 2 mm, and a curing agent ratio of 9:1.

4.2 Relationship between Porosity and Mechanical Deformation Behavior

The tensile specimens shown in Fig. 5 were produced in nine cases of the L9 orthogonal array table according to the process parameters in Table 3, and a tensile test was conducted at the speed of 10 mm/s using a small tensile tester (JSV-100 model, Algol Co., Taiwan) that can load a maximum weight of 100 N.

Fig. 8 shows the relationship between porosity, tensile load, and deformation until fracture. Because each tensile test uses three kinds of sheet thickness, there is a difference in the load applied. Comparing the porosity and deformation of the specimens having the same thickness, the larger the porosity, the more flexible the specimen and the more increase of the deformation until the fracture.

Case 2, with the powder particle size of less than 150 μm , and a specimen thickness of 4 mm, showed the highest deformation. However, in Case 3, where the thickness of the specimen is 6 mm, the overall porosity was the highest. However, as

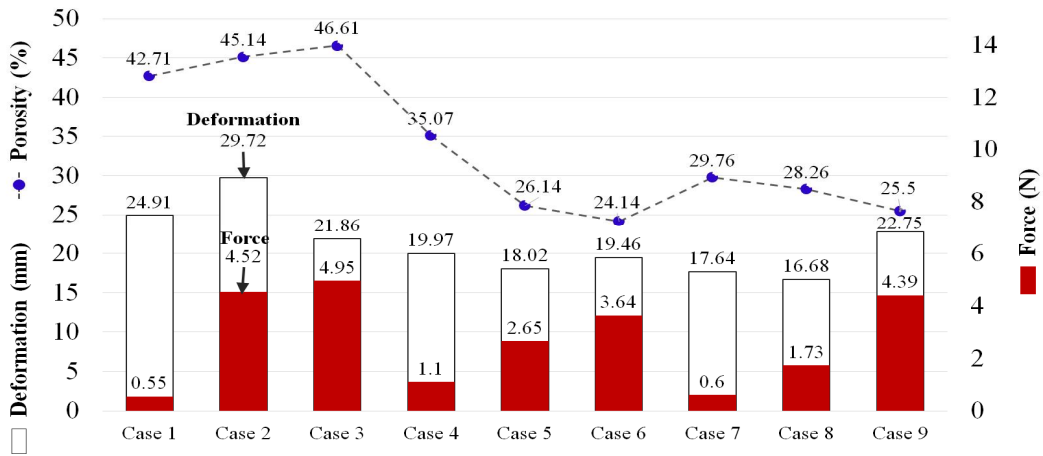


Fig. 8 Relationship between tensile deformation and porosity of porous sheet

described above, the fracture occurred rather easily because of the unevenness of the local physical properties. In other cases (e.g., Cases 6 and 9) with the specimen thickness of 6 mm, it was found that the amount of deformation was also not significant.

In this experiment, it was difficult to precisely control the pores in the specimen. Therefore, there was a problem of big deviation and error of the specimen. However, when the specimens have the same thickness, it was found that the larger the porosity, the higher the flexibility and the more increase of the deformation until fracture. Therefore, this study found that it is important to maximize the porosity of the porous sheet, and make it thin for flexible device application.

5. Conclusion

This study proposed a process of producing porous sheets using water-soluble powders and PDMS, and developed the following conclusions through factor-effect analysis of process parameters and mechanical deformation behavior:

1. As a result of the Taguchi factor-effect analysis,

it was found that the smaller the size of the water-soluble particle, the better it is for improvement of porosity. The porosity is more influenced by the size of the water-soluble particles than other process parameters. This study used sugar powder of 150 μm or less and got the highest porosity with the thin sheet.

2. It was found that the larger the porosity, the more flexible the specimen becomes, causing the tensile deformation to increase until fracture. However, fracture occurred even in a small amount of deformation, regardless of overall porosity increase, because it is difficult to obtain a uniform pore distribution if the thickness of the specimen increases.
3. Therefore, in the case of a porous sheet to be applied to a flexible device, it was found that a porous substrate with a high porosity and a small thickness is more advantageous for increasing flexibility.
4. Further research on mathematical model development, a method of porosity increase, and a method of producing a specimen with uniform pore distribution need to be conducted in the future for water-soluble powder mixture forms.

Acknowledgment

“This paper is a basic research project (No.2017R1D1A1A09000923) supported by the National Research Foundation of Korea in 2017 and a research paper (No.N0000990) partly funded by the Ministry of Trade, Industry and Energy with the support from the Engineering Development Research Center”

REFERENCES

1. Bobbert, F. S. L. and Zadpoor, A. A., “Effects of Bone Substitute Architecture and Surface Properties on Cell Response, Angiogenesis, and Structure of New Bone,” *Materials Chemistry B*, Vol. 5, pp. 6175-6192, 2017.
2. Yan, D. X., Ren, P. G., Pang, H., Yang, M. B. and Li, Z. M., “Efficient Electromagnetic Interference Shielding of Lightweight Graphene/Polystyrene Composite,” *Materials Chemistry*, Vol. 22, pp. 18772-18774, 2012.
3. Choi, S. J., Kwon, T. H., Im, H. W., Moon, D. I., Beak, D. J., Seol, M. L., Duarte, J. P. and Choi, Y. K., "A Polydimethylsiloxane (PDMS) Sponge for the Selective Absorption of Oil from Water," *ACS Applied Materials Interfaces*, Vol. 3, pp. 4552-4556, 2011.
4. King, M. G., Baragwanath, A. J., Rosmond, M. C., Wood, D. and Gallant, A. J., "Porous PDMS Force Sensitive Resistors," *Procedia Chemistry*, Vol. 1, pp. 568-571, 2009.
5. Kuanh, J., Lui, L., Gao, Y., Zhou, D., Chen, Z., Han, B. and Zhang, Z., “A Hierarchically Structured Graphene Foam and its Potential as a Large-Scale Strain-Gauge Sensor,” *Nanoscale*, Vol. 5, pp. 12171, 2013.
6. Xu, M., Qi, J., Li, F. and Zhang, Y., “Highly Stretchable Strain Sensors with Reduced Graphene Oxide Sensing Liquids for Wearable Electronics”, *Nanoscale*, Vol. 10, pp. 5264-5271, 2018.
7. Fee, C., “3D-Printed Porous bed Structure,” *Current Opinion in Chemical Engineering*, Vol. 18, pp. 10-15, 2017.
8. Zocca, A., Gomes, C. M., Staude, A., Bernardo, E. and Colombo, P., “SiOC ceramics with ordered porosity by 3D-printing of a preceramic polymer,” *Materials Research Society*, Vol. 28, No. 17, pp. 2243-2252, 2013.
9. Li, Z. X., Ye, L. J., She, J. Q., Xie, K. Y. and Li, Y. J., “Strain-gauge Sensing Composite Films with Self-restoring Water-repellent Properties for Monitoring Human Movements,” *Composites Communications*, Vol. 7, pp. 23-29, 2018.
10. Prakasam, M., Popescu, M., Piticescu, R. and Largeteau, A., “Fabrication Methodologies of Biomimetic and Bioactive Scaffolds for Tissue Engineering Applications,” *Technologies and Clinical Applications*, Chapter 1, 2017.
11. Langley, D., Giusti, Gael., Mayousse, C., Celle, C., Bellet, D. and Simonate, J. P. “Flexible Transparent Conductive Materials Based on Silver Nanowire Networks : a review,” *Nanotechnology*, Vol. 24, pp. 452001, 2013.
12. Khanafer, K., Duprey, A., Schlicht, M. and Berguer, R., "Effects of Strain Rate, Mixing Ratio, and Stress-Strain Definition on the Mechanical Behavior of the Polydimethylsiloxane (PDMS) material as related to its Biological Applications," *Biomedical Microdevices*, Vol. 11, pp. 503-508, 2009.
13. ASTM International(2016), "ASTM D412-16, Standard Test Methods for Vulcanized Rubber and Thermoplastic Elastomers—Tension," Retrieved 2016, from <http://www.astm.org/cgi-bin/resolver.cgi?D412-16>.
14. Fung, C., P. and Kang, P., C., "Multi-response Optimization in Friction Properties of PBT Composites using Taguchi Method and Principle component analysis," *Journal of Materials Processing Technology*, Vol. 170, pp. 602-610, 2005